European Journal of Molecular & Clinical Medicine

ISSN 2515-8260 Volume 08, Issue 03, 2021

Study Of Stress And Thermo-Optic In Photonic Crystal Fiber Laser With Tow End Pump Scheme

Mostafa Abouricha [1,*] , Anas El Kasmi[2], Said Amrane[3] , Abdelkader Boulezhar [2] and Ali. Nassiri[4]

[1]EPTHE, Department of Physics, Faculty of Sciences, Ibn Zohr University of Agadir BP 8106, Morocco.

[2]LRESD, Department of Physics, Faculty of Sciences Ain-chock Hassan II University of Casablanca, BP 20100, Morocco.

[3]INPT Optics Lab,National Institute of Posts and Telecommunications, Rabbat, Morocco.

[4]Laboratoire de Métrologie et Traitement de l'Information Faculty of sciences Ibn Zohr University BP 8106 – Agadir, Morocco.

{M. Abouricha}m.abouricha@uiz.ac.ma

Keywords: ***Pump Schemes, Stress optic, Yb-Doped Fiber Lasers, Thermal Effects in Fiber Lasers, Birefringence, change in index of refraction***

Abstract:*In this paper, we present a study of thermal, change in index of refraction and stress in photonic crystal fiber (PCF) lasers with the tow-end pump scheme. We show the effect of the tow-end pump scheme, small length of fiber and the large radius fiber on the beam quality is the most suitable choice compared to large length and small radii of fiber. In addition, we show that management of thermal effects in (PCF) lasers will success of scaling up efforts and determine the efficiency.*

1 INTRODUCTION

The photonicscrystal fiberlasers and gas lasers make Yb^{3+} doped, hasbenn the subject of theseveralresearches reported [1-6]. With the new type of the pump schemes with the high brightness semiconductor diode pump laser was studied [7]. And the different type of photonic crystal fibers (PCFs) is attracting increasing interests because of its unique properties such as endlessly single-mode guiding, freedom of dispersion characteristics, and large mode area [8-9]. We also concentrate on PCFs in which a core doped with Yb^{3+}(region 1) surrounded by a lower index cladding (region 2), which is, surrounded by an air-clad region (region 3), in turn, surrounded by a second lower index cladding index (region 4).

Using the numerical calculation and the finite-difference method (FDM) and shootingMethodto solve the rate equations[10], in order to find the distributions of the pump and signal power and from these last we can find the heat dissipation in the PCF laser

, we have determined the expressions of temperature in different regions of the photonic crystal fiber laser (PCF) along the axial and radial directions from the integration of the steady-state heat equation for an isotropic medium. Then we used the expressions previously derived for the temperatures in all

Regions core (1), clad (2), air-clad (3), and outer clad(4) [4,11] in the results of the expressions for the stress components ($\sigma_z(r)$, $\sigma_\varphi(r)$ and $\sigma_r(r)$) in regions core (1), clad (2), air-clad (3), and outer clad (4). The results are compared in radius and length of fiber, for giving the design guidelines saving pump powers andto ensure maximum heat dissipation. The calculated stress values are very small in tow end pump scheme, will consequently have a negligible effect upon the index of refraction, and limitations due to thermo-optical effects or fracture damage of the fibre.

The thetow-end pump scheme, the values of stress is between -0.5×10^{-6} kg/m^2 and -4.6×10^{-6} kg/m^2. Therefore, the values of the change in index of refraction increases in the short length and decreases in the big radius. In addition, these values remain small compared to conventional fiber.

2 AVERAGE TEMPERATURE IN PCF LASER

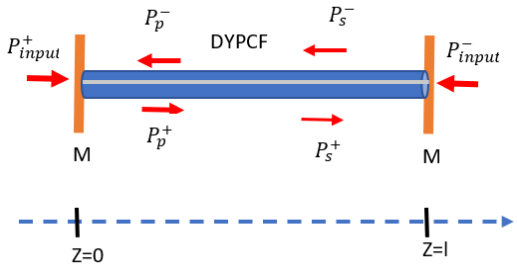

Figure 1: Schematic illustration of the pump scheme in PCF.

As shown in Fig 1, a typical high power Yb^{3+} doped double-clad PCF laser consists of an Yb^{3+} doped dou- ble PCF with reflectors on both of the ends.

Fig 2 shows the heat flow mechanisms in PCF laser and the radial coordinate r and the tangential angle φ. The quantities r_1,r_2, r_3 and r_4 are the core, inner cladding, air-clad and outer cladding radii, respectively.

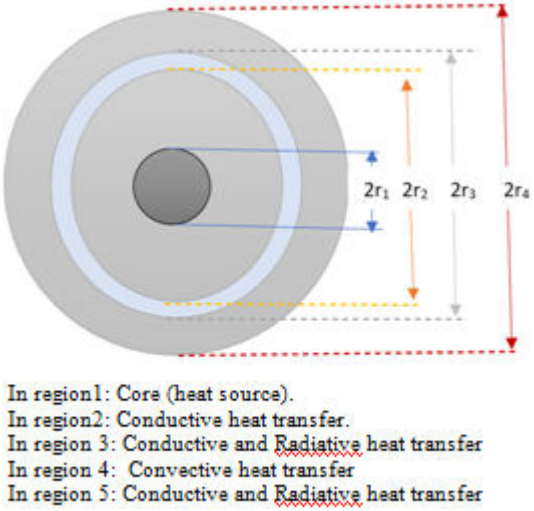

Figure 2: Heat transfertmechanisms in PCF laser.

Fig. 2 illustrates the heat dissipation model of PCF demonstrating the heat transfert procedure from the fiber core to the ambient air. The heat dissipation procedure can be divided in[10]:

The expression of temperature in a fiber reported in [11] is necessary for determining the radially varying index of refraction due to variation of temperature dT, the calculated stresses, and the change in index of refraction through the stress-optic effect.
We start by calculation the average temperature Tavas[12]:

$$T_{av} = \frac{\int_0^{r_1} T(r)dr + \int_{r_1}^{r_2} T(r)dr + \int_{r_2}^{r_3} T(r)dr + \int_{r_3}^{r_4} T(r)dr}{\int_0^{r_4} T(r)dr} \quad (1)$$

Where the temperature expressions $T_1(r)$,$T_2(r)$, $T_3(r)$ and $T_4(r)$ are reported[9].

3 STRESS DISTRIBUTIONS

Because length of the optical fibers is much greater than a typical fiber outside radius (r_4), we can invoke the plane-strain approximation [13] in which the z strain everywhere. The radial, tangential, and z stresses $\sigma z(r)$, $\sigma_r(r)$, and $\sigma_\varphi(r)$ can be found from [13].

$$\sigma_r(r) = \frac{\alpha E}{(1-\mu)}\left[\frac{1}{{r_4}^2}\int_0^{r_4} rT(r)dr - \frac{1}{r^2}\int_0^{r} rT(r)dr\right] (2)$$

$$\sigma_\varphi(r) = \frac{\alpha E}{(1-\mu)}\left[\frac{1}{{r_4}^2}\int_0^{r_4} rT(r)dr + \frac{1}{r^2}\int_0^{r} rT(r)dr - T(r)\right] \quad (3)$$

We considerthat there is no traction in the outerfaces of the fiber therefore:

$$\sigma_z(r) = \sigma_r(r) + \sigma_\varphi(r) \quad (4)$$

Where α,*v* and Eare thermal expansion coefficient,Poisson's ratio, andYoung's modulus, respectively. Using the expressions previously derived for the temperatures in Regions 1, 2, 3, and 4 [11], Solution of (2)-(3), results in the following final expressions for the stresses in allregions core 1, clad 2, air-clad3, and outer clad 4:
It can be shown the satisfy of the boundary conditions as:

$$\sigma_r^4(r = r_4) = 0,\ \sigma_r^1(r = 0) = \sigma_\varphi^1(r = 0),\ \ \sigma_\varphi^4(r = r_4) = \sigma_z^4(r = r_4)$$

And the continuity conditions as:

$$\sigma_z^1(r = r_1) = \sigma_z^2(r = r_1),\ \sigma_r^1(r = r_1) = \sigma_r^2(r = r_1),\ \ \sigma_\varphi^1(r = r_1) = \sigma_\varphi^2(r = r_1),\ \sigma_z^2(r = r_2) = \sigma_z^3(r = r_2),\ \sigma_r^2(r = r_2) = \sigma_r^3(r = r_2),\ \ \sigma_\varphi^2(r = r_2) = \sigma_\varphi^3(r = r_2),$$

$$\sigma_z^3(r = r_3) = \sigma_z^4(r = r_3),\ \sigma_r^3(r = r_3) = \sigma_r^4(r = r_4)\ \text{and}\ \sigma_\varphi^3(r = r_3) = \sigma_\varphi^4(r = r_3),$$

We will use these equations to calculate the radial variation of the refractive index tow end pump scheme, due to the stress-optic effect. Note that the equations as derived above for the fiber stresses could also have been obtained by use of the deviation of the temperature distribution from the average and the Airy stress potential [13].

ISSN 2515-8260 Volume 08, Issue 03, 2021

4 INDEXE OF REFRACTIONS

Using the expressions for the radial temperature distributions, reported [9] and for the stress distributions reported in [4], we tray now to make calculation of the radially varying radial and tangential index of refraction distributions. For comparison in different pump schemes, we prefer to cast the calculation of the induced change in the index of refraction in terms of material stresses, rather than strains. We begin by writing the changes in the indices of refraction[15,16]

$\Delta n_{r,\varphi}^{1,2,3,4}(r) = \Delta n_{r,\varphi}^{1,2,3,4} - n_0 = \Delta n_{\beta}^{1,2,3,4}(r) + \Delta n_{ST,r,\varphi}^{1,2,3,4}(r)$ (5)

Where

$\Delta n_{\beta}^{1,2,3,4}(r)$ change in index due to change in index with temperature ($\frac{dn}{dT}$).

$n_O = 1.45$

$\Delta n_{r,\varphi}^{1,2,3,4}(r)$ Stress-induced index changes for the radial r and tangential φ components of the electric field. Here, we will calculate $\Delta n_{\beta}^{1,2,3,4}(r)$ using the following equation:

$\Delta n_{\beta}^{1,2,3,4}(r) = \beta(T_{1,2,3,4}(r) - T_c)$ (6)

5 DISCUSSIONS

5. 1 Stress Effect

In Figures 3, we plotted the stress components longitudinal as a function of the radial coordinate r for a YPCF with a pump of 200 W, r_4 = 300 µm is the outer radius, convective coefficient h = 40.9 W.K/cm^2. The quantities $B_{\perp}$ and $B_{\parallel}$ are known in the optics and laser literature as the perpendicular and parallel stress-optic coefficients their values are $27.7 \times 10^{-8} cm^2/kg$ and $4.5 \times 10^{-8} cm^2/kg$ and the thermal expansion coefficient is $\alpha = 0.51 \times 10^{-6} K^{-1}$[17]. The numerical value of E and $\nu$are $73GPa$ and $\nu = 0.164$ [14], we show the value of stress is very small in this case the pump scheme. In addition, we observed that the stress value isminimal in the center of the cavity. Therefore, we propose a solution to minimize the variation of the refractive index variation, a multipoint pump scheme. However, concerning the tangential component $\sigma_{\varphi}(r)$, the increase is less rapid. We notice that all required boundary conditions are satisfied.

5. 2Index Of Refraction

Using the expressions of the variation of refractive index reported in [4] , we plotted the tangential and the radial indices of refraction as a function of the radial coordinate r in different pump schemes, Fig 4, the pump power used is 200 W, the fiber outside radius is r_4 = 300 µm,. The curves for $\Delta n_{\varphi}(r)$ and $\Delta n_r(r)$are identicalin r = $r_4$and in r = 0 µm. Nevertheless, in Fig. 4the value is in order of 3×10^{-3} to 7×10^{-3}.We notice in side of pumping there is a small difference of the variationof refractive index between the outer clad fiber r=r_4 and the core .

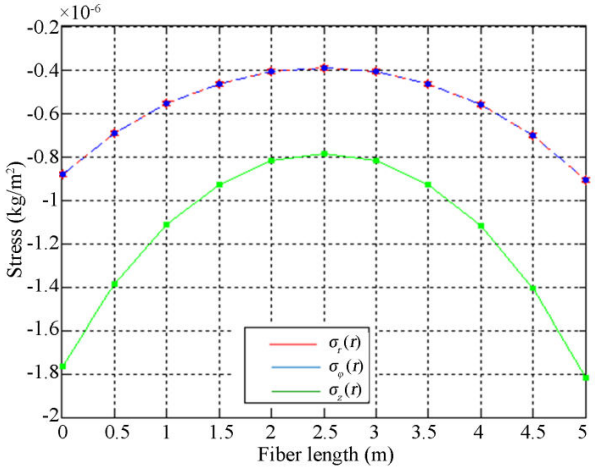

Figure 3: Evolution longitudinal of the stress in PCF at 100 W pump of 940 nm load calculated by FDM analysis and shooting method withtow-end pump scheme.

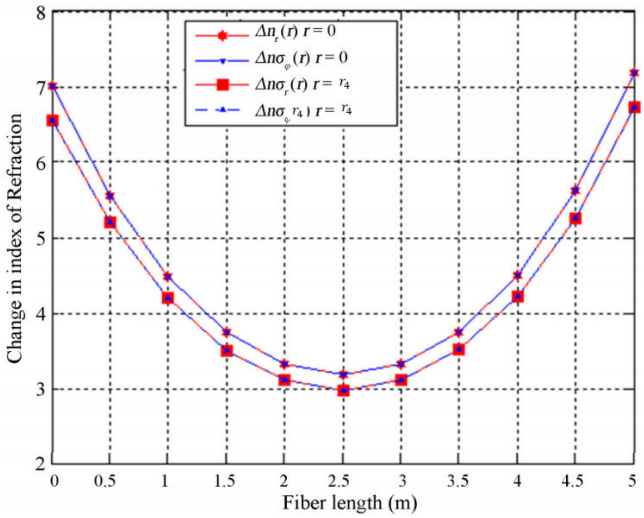

Figure 4: The change in index of refraction in PCF at 100 W pump for each side, load calculated by FDM analysis and shoting method with tow-end pump schemes.

6 CONCLUSION

In conclusion, we have investigated of the thermo-optic and the stress in a photonic crystal fiber (PCFs) in tow-end pump scheme. Using in these calculations a simple model of (PCFs) and the finite differential method (FDM) and the shooting method, we have revealed the temperature in the core of the fiber and by laws of heat transfer, we determined its value at the surface of the fiber and the stress value in the different regions of the fiber. In conclusion, regarding thermo-optic, stress and the change in index of refraction, their value does not have a great effect on the quality of the laser beam in different length of the cavity, especially in the small cavity with tow end pump scheme and multipoint pump scheme. Hence, after this investigation, we proved the architecture of PCF laser cavity that was the most suitable in special uses and a specific condition.

7 REFERENCES

[1] J. Limpert, A. Liem, H. Zellmer and A. Tunnerman, "500 W Continuous-Wave Fiber Laser with Excellent Beam Quality," Electronics Letters, Vol. 39, No. 8, 2003, pp. 645-647.

[2] D. L. DiGiovanni and M. H. Muendel, "High power fiber lasers and amplifiers," Opt. Photon. News, pp. 26–30, Jan. 1999.

[3] N. Platonov, V.P. Gapontsev, O. Shkurihin, and I. Zaitsev, "400W low-noise single-mode CW Ytterbium fiber laser with an integrated fiber delivery," in Conference on Lasers and Electro-Optics (Optical Society of America, Washighton, D.C., 2003), postdeadline paper CThPDB9.

[4]M.Abouricha, M., et al. (2014) Theoretical and Numerical Study of Stress and Thermo-Optic in Photonic Crystal Fiber Laser in Different Pump Schemes. Open Journal of Metal, 4, 120-130.

[5] M. H. Muendel, "High-power fiber laser studies at the polaroid corporation," in Proc. SPIE Conf. High-Power Lasers San Jose, CA, 1999, vol. 3264, pp. 21–29.

[6] L. Shang, "Comparative Study of the Output Characteris- tics of Ytterbium-Doped Double-Clad Fiber Lasers with Different Pump Schemes," Optik, Vol. 122, No. 21, 2011, pp. 1899-1902.

[7] J.C Knight, P. St. J. Russell, New ways to guide light, Science 296 (2002) 276-277

[8] J.C Knight, T. A. Briks, R. F. Cregan, et al., Large mode area Photonic Crystal Fiber, Electron. Lett. 34 (1998) 1347-1349.

[9] M. Abouricha, A. Boulezhar, N. Habiballah, '' The Comparative Study of the Temperature Distribution of Fiber Laser with Different Pump Schemes'' Open Journal of Metal, 2013, 3, 64-71

[10] I. Kelson and A. Hardy, "Srongly Pumped Fiber Lasers," IEEE Journal of Quantum Electronics, Vol. 34, No. 9, 1998, pp. 1570-1577. http://dx.doi.org/10.1109/3.709573

[11] J. Limpert, T. Schreiber, A. Liem, S. Nolte, H. Zellmer ''Thermo-optical properties of air-clad photonic crystal fiber lasers in high power operation'' 3 November 2003 / Vol. 11, No. 22 / OPTICS EXPRESS 2984.

[12] B. A. Boley and J. H. Weiner, Theory of Thermal Stresses, reprint ed. Melbourne, FL: Kreiger, 1985.

[13] David C. Brown, Member, IEEE, and Hanna J. Hoffman ''Thermal, Stress, and Thermo-Optic Effects in High Average Power Double-Clad Silica Fiber Lasers'' IEEE JOURNAL OF QUANTUM ELECTRONICS, VOL. 37, NO. 2, FEBRUARY 2001 207

[14] J. M. Eggleston, T. J. Kane, K. Kuhn, J. Unternahrer, and R. L. Byer, "The slab geometry laser—Part I: Theory," IEEE J. Quantum Electron., vol. QE-20, pp. 289–301, 1984.

[15] Handbook of Optics (Sponsored by the Optical Society of America), vol. II, Devices, Measurements, and Properties, M. Bass, Ed., McGraw-Hill, New York, 1995.

[16] , "Nonlinear Thermal Distortion in YAG rod amplifiers," IEEE J. Quantum Electron., vol. 34, pp. 2383–2382, 1998.

[17] W. F. Krupke, M. D. Shinn, J. E. Marion, J. A. Caird, and S. E. Stokowski, "Spectroscopic, optical, and thermomechanical properties of neodymium- and chromium-doped gadolinium scandium gallium garnet," J. Opt. Soc. Amer. B, vol. 3, pp. 102 113, 1986.